

Structural and Physical Properties of Y- doped BiFeO₃ Material Prepared by Sol-gel Method

Dao Viet Thang^{1,2,*}, Du Thi Xuan Thao², Nguyen Van Minh¹

¹*Center for Nano science and Technology, Hanoi National University of Education,
136 Xuan Thuy, Hanoi, Vietnam*

²*Department of Physics, University of Mining - Geology, Dong Ngac, Tu Liem, Hanoi, Vietnam*

Received 19 July 2013

Revised 23 August 2013; Accepted 20 September 2013

Abstract: Y - doped BiFeO₃ materials were prepared by a sol – gel method. X-ray diffraction (XRD) measurement has been carried out to characterize crystal structure and to detect the impurities existing in these materials. The results showed that both lattice constants a and c of the unit cell of BiFeO₃ substance become smaller as the Y³⁺ content is increased. The effect of introducing Y³⁺ was to decrease the optical band gap for doped samples Bi_{1-x}Y_xFeO₃ (x = 0.00 ÷ 0.20). Magnetic properties of Y-doped BiFeO₃ were investigated by vibrating sample magnetometer (VSM) measurements at room temperature, using maximum magnetic field of about 10 kOe. These materials exhibited a weak ferromagnetic behavior and magnetization of the sample was improved as presence of Y³⁺ ions. When x = 0.15, 0.20, structural and magnetic properties change sharply. Y doping BiFeO₃ material modifies its physical properties.

1. Introduction

Ferroelectromagnetic materials, multiferroics, exhibit ferroelectric properties in combination with the ferromagnetic properties [1]. Additionally they exhibit the phenomenon called magnetoelectric coupling, magnetization induced by an electric field and electric polarization in a magnetic field. Recently, partial substitution of Bi³⁺ ions by lanthanides has been shown to improve ferroelectric properties and magnetization [2–3]. Zhang *et al.* [4] and Das *et al.* [3] suggested that La³⁺ substitution for Bi³⁺ eliminates impurity phases and destroys the cycloidal spin structure resulting in uniform canted antiferromagnetic ordering. Zhang also reported that the structure changes from rhombohedral to orthorhombic at 30 mol% La. In the studies on dopant effects of Sm reported by Nalwa *et al.* [2] and Yuan [5] and those of Nd reported by Yuan *et al.* [6] in BiFeO₃, changes in the crystal structure of the materials were observed, which resulted in improving piezoelectric properties, long-range

* Corresponding author. Tel.: 84-985811377
Email: dvthangphysics@gmail.com

ferroelectric and canted antiferromagnetic orders. On the other hand, Uniyal and Yadav [7] claimed that 10 mol% Gd substituted for bismuth in the sample compound did not change the crystal structure but only reduced the volume fraction of impurity phases, while decreasing the Neel temperature T_N from 370 °C to 150 °C, and enhancing the magnetization to the extent of allowing the generation of the ferroelectric hysteresis loops [7]. The report of Hou Zhi – Ling *et al.* [8] shown that demonstrates the lattice contraction and magnetic properties improved due to 5 mol% Y substituted for bismuth. Our report shows effect of Y - doping on structure and physical properties of $\text{Bi}_{1-x}\text{Y}_x\text{FeO}_3$ ($x = 0.00 \div 0.20$) materials. In this paper, we choose Y-content from $x = 0.00$ to $x = 0.20$ because of two reasons (i) with x small, the properties of Y doping have no significant changes; (ii) with $x > 0.20$, it may attribute to structural transition from rhombohedral (R_{3c}) to orthorhombic (P_{nma}) by Y substitution [9]

2. Experimental

Multiferroic $\text{Bi}_{1-x}\text{Y}_x\text{FeO}_3$ ($x = 0.00 \div 0.20$) powders have been synthesized by a sol – gel method. The chemicals used to create the samples are ferric nitrate $\text{Fe}(\text{NO}_3)_3 \cdot 9\text{H}_2\text{O}$, bismuth nitrate $\text{Bi}(\text{NO}_3)_3 \cdot 5\text{H}_2\text{O}$, yttrium nitrate $\text{Y}(\text{NO}_3)_3 \cdot 6\text{H}_2\text{O}$, citric acid and ethylene glycol. In the first step, these chemicals were mixed in correct weight contribution and an aqueous solution of citric acid was prepared in distilled water. Then ferric nitrate, bismuth nitrate and yttrium nitrate were added in turn with constant stirring at temperature 50 – 60 °C to avoid precipitation and obtain a homogeneous mixture. Now ethylene glycol was added into the solution with citric acid/ethylene glycol ratio of 70/30. After that water was evaporated at temperatures 100 °C to obtain colloidal gel bath. Finally, the gel was heated at temperatures of 700 °C for 6 hours to remove organics in the samples.

The samples were characterized by using different techniques. X-ray diffraction diagrams was used for phase identification and crystal structural analysis. The optical properties and electrical properties were determined by the absorption spectra. Vibrating sample magnetometer was used to measure the magnetic properties of the samples.

3. Results and discussion

Figure 1a shows the X-ray diffraction patterns of $\text{Bi}_{1-x}\text{Y}_x\text{FeO}_3$ samples ($x = 0.05 \div 0.20$). The XRD patterns are in excellent accordance with the powder data of JCPDS Card No. 71-2494 for BiFeO_3 crystals. Generally, for all samples, the second phase peaks attributed to Fe or Bi rich phases $\text{Bi}_2\text{Fe}_4\text{O}_9$ and $\text{Bi}_{25}\text{Fe}_{40}$ (asterisk in Fig. 1a) were routinely observed as shown in previous results [10]. While Y substituted at the Bi site, the phase impurities can not be observed. However, with increasing Y content, another phase $\text{Y}_3\text{Fe}_5\text{O}_{12}$ appears in the $x = 0.10, 0.15$ and 0.20 powder samples [11]. For Y-doped BiFeO_3 , all peaks are indexed according to the R_{3c} cell of BiFeO_3 . The lattice parameters deduced for pure BiFeO_3 rhombohedral unit cell were found to have values $a = 5.587 \text{ \AA}$ and $c = 13.872 \text{ \AA}$. The results showed that both lattice constants a and c of the unit cell of BiFeO_3 substance become smaller as the Y^{3+} content is increased in the figure 1b. It is because the Y^{3+} ion radius (1.02

\AA) is smaller than that of Bi^{3+} ion (1.17\AA) [12]. Crystallite size (d) was evaluated using the well-known Sherrer formula $d = 0.94\lambda / (\beta \cos\theta)$ [12, 13], where β is the full width at half-maximum of the chosen diffraction line (here we have chosen (012), (104), (110) and (024) intense peaks), θ the Bragg diffraction angle and λ the wavelength of $\text{CuK}\alpha$ radiation (1.5406\AA). The result is shown in figure 1b. The crystalline size is about 46 nm for pure sample and decreases as Y-doping is increased from $x = 0.00$ to 0.20 , which is attributed to the smaller ion radius of Y^{3+} than that of Bi^{3+} [8].

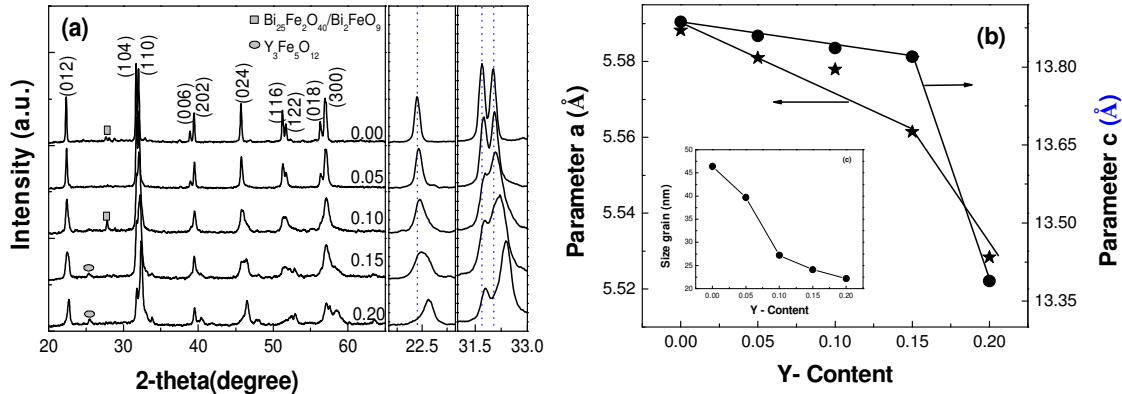


Figure 1. (a) XRD patterns of $\text{Bi}_{1-x}\text{Y}_x\text{FeO}_3$ powders; (b) a, c structure parameters depend on the Y content; and the insert shows average crystallite size depend on the Y content.

Figure 2 shows the Raman scattering spectroscopy of $\text{Bi}_{1-x}\text{Y}_x\text{FeO}_3$ samples ($x = 0.00 \div 0.20$) measured at room temperature. The previous report has shown that the Raman active modes of the rhombohedral (R_{3c}) BiFeO_3 can be summarized using the following irreducible representation: $\Gamma = 4A_1 + 9E$ [12-14]. In present study we have observed $4A_1$ modes (at wavenumbers of 170, 210, 464, and 549 cm^{-1}) and $6E$ modes (at wavenumbers of 134, 256, 281, 340, 368, and 517 cm^{-1}). The intensities of E modes are greater than that of A_1 modes in the present study. Since Raman scattering spectroscopy is sensitive to atomic displacements, the evolvement of Raman normal modes with increasing Y content can provide valuable information about ionic substitution and electric polarization. The stereochemical activity of the Bi electron pair plays major role in the change, both in Bi-O covalent bonds and characteristic modes observed at 170, 210, 256, 281, 340 and 368 cm^{-1} for pure BiFeO_3 . These modes are supposedly believed to be responsible for the ferroelectric nature of the bismuth ferrite samples [15-16]. With increasing in substitution ions, there is a change of Bi-O covalent bonds as a result of the decline in the stereochemical activity of the Bi lone electron pair and thus in long range ferroelectric order. If the mode frequency is governed by local factors, such as the force constant and ionic mass it will be proportional to $(k/M)^{1/2}$, where k is the force constant and M is the reduced mass [13]. Since ionic radius of Bi^{3+} is similar to Y^{3+} , k is assumed to be independent of substitution ions. However, the shifting of Raman modes at higher frequencies, attrition of the prominent modes and the change in crystal structure is likely due to the A-site disorder created by Y substitution, having lower atomic weight 88.9 g as compared to $\text{Bi } 209.0 \text{ g}$.

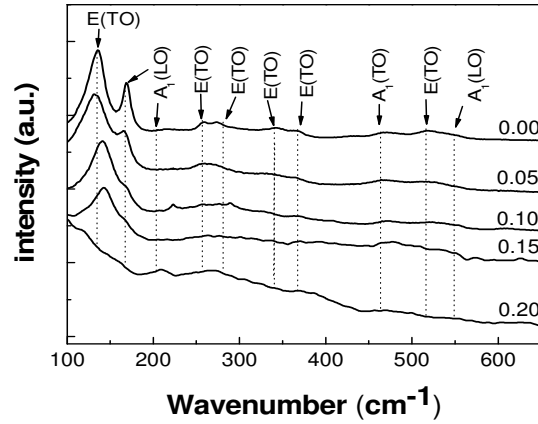


Figure 2. Raman scattering spectra of $\text{Bi}_{1-x}\text{Y}_x\text{FeO}_3$ materials ($x = 0.00 \div 0.20$) at room temperature.

The UV–Vis absorption spectra of the $\text{Bi}_{1-x}\text{Y}_x\text{FeO}_3$ materials were showed in Fig. 3a. In the previous research, using chemical methods Zhike Liu *et al.* reported particle size of $150 \div 200$ nm and the optical band gap (E_g) material of about 2.10 eV for BiFeO_3 [17]; approximate values of optical band gap were observed on BiFeO_3 thin films [18-19]; Theoretical calculations of Fan *et al.* showed BiFeO_3 material have the optical band gap to 2.5 eV [20]. By analyzing the absorption spectra (in Fig. 3a), we can obtain the values of optical band gap in the range of 2.01 \div 2.08 eV. In the guide to eyes, E_g decreases with increasing the Y-doped content. The insert in Fig. 3b shows a plot of $(\alpha h\nu)^2$ as a function of photon energy. Analysis of the density of states indicated that the valence band was consisted with Fe-d and O-p states, and the conduction band was composed of Fe-d and Bi-p states [17]. Outside the absorption spectrum also shows the absorbance at 700 nm position receptors. This may be related to minor absorption happens when the electron is excited from t_{2g} bands to e_g bands [20].

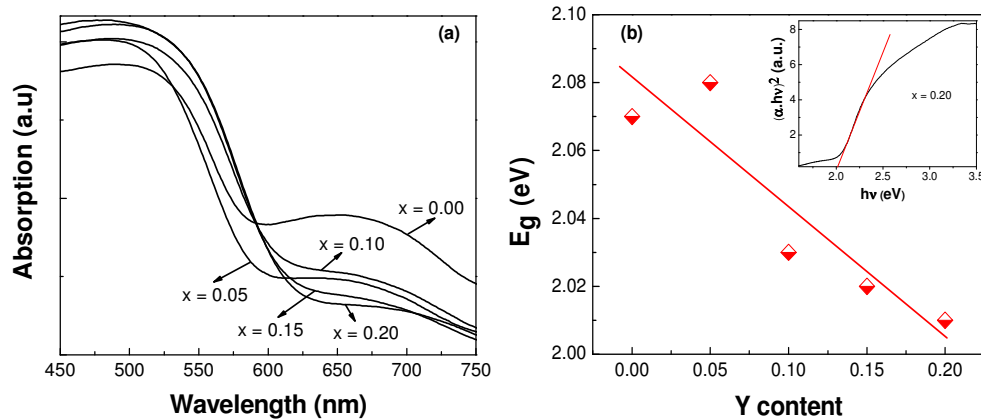


Figure 3. (a) UV–Vis absorption spectra of the $\text{Bi}_{1-x}\text{Y}_x\text{FeO}_3$ ($x = 0.00 \div 0.20$) materials; (b) the optical band gap of samples and insert shows a plot of $(\alpha h\nu)^2$ as a function of photon energy.

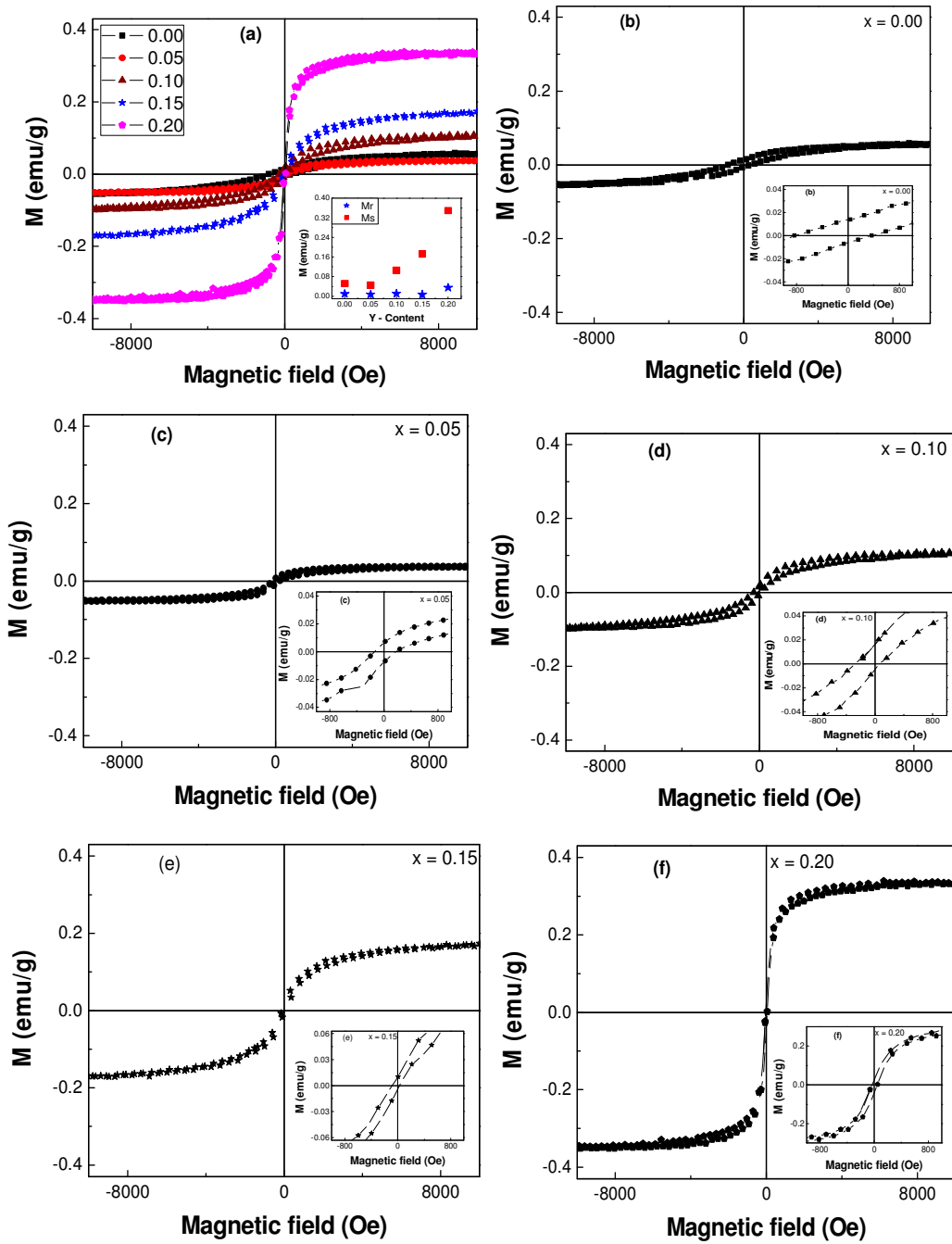


Figure 4. Room-temperature magnetization hysteresis loops of Bi_{1-x}Fe_xO₃ powders with x = 0.00 ÷ 0.20 for (b) – (f) and the insert saturation magnetization (Ms) and remnant magnetization (Mr) versus x value (a).

The magnetization-magnetic field (M-H) curves of $\text{Bi}_{1-x}\text{Y}_x\text{FeO}_3$ powders measured with a maximum magnetic field of 10 kOe, as shown in Fig. 4. The partly enlarged curves are shown in the corresponding insert. In fact, BiFeO_3 is known to be antiferromagnetic having a G-type magnetic structure [21], but has a residual magnetic moment due to a canted spin structure (weak ferromagnetic) [22]. However, the Y-doped specimens exhibited a magnetic hysteresis loops, referring to a ferromagnetic behavior. As shown in Fig. 4, the curves are clearly not colinear. The saturation magnetization (M_s) are 0.052, 0.045, 0.106, 0.172 and 0.349 emu/g for samples $x = 0.00, 0.05, 0.10, 0.15$ and 0.20 , respectively. The remnant magnetizations (M_r) are 0.010, 0.007, 0.011, 0.007 and 0.035 emu/g, respectively. The M_s and M_r values as the function of x are plotted in the insert of Fig. 4a. A relevant research [23] reported that the Y-substitution could suppresses the spin cycloid of BiYFeO_3 . Further analysis reveals that the M_s and M_r values of $\text{Bi}_{1-x}\text{Y}_x\text{FeO}_3$ with $x = 0.15$ and 0.20 are significantly bigger than those of others, suggesting that with smaller value of $x = 0.10$. The Y-substitution can only suppress but can not destruct the spin cycloid, which is responsible for the limited and smooth increase of the M_s and M_r values. However, when $x \geq 0.10$, the Y substitution results spin cycloid, so that the latent magnetization locked the cycloid may be released, and a significant increasing of M_s and M_r value is observed. Another phase, such as $\text{Y}_3\text{Fe}_5\text{O}_{12}$ can also be found evidently, which may contribute to the increasing of magnetization value, it is consistent with predictions in reports of Feng *et al.* [11]. The reports of Hou Zhi-Ling *et al.* [8] had shown the Y ions, occupying the lattice sites, resulted in the changes of Fe-O-Fe bond angles which affected the super exchange Fe-O-Fe interactions. Although the Y-doping element does not contain 4f electrons, a small amount of doping can induce a strong magnetization [8]. In reports of Luo *et al.* [24] $\text{Bi}_{1.04-x}\text{Y}_x\text{FeO}_3$ ($0.00 < x < 0.30$) ceramics were synthesized by method, results showed that with $x < 0.20$ remnant magnetization and saturate magnetization have no significant changes. With increasing x up to 0.30 , a clear hysteresis loop can be observed, indicating the ferromagnetic properties. The saturate magnetization ($M_s = 0.31$ emu/g) of $\text{Bi}_{0.74}\text{Y}_{0.30}\text{FeO}_3$ increases significantly compared to those values of BiFeO_3 and has been attributed to structural transition from rhombohedral (R_{3c}) to orthorhombic (P_{nma}) [24]. The difference in our report, with increasing x up 0.20 no structural transition, the saturate magnetization ($M_s = 0.349$ emu/g). This results are good for the application of Y-doped BiFeO_3 materials. For Y-substitution can improve the saturation magnetization so much should be discussed more and another effective analytical method should be introduced to assist.

4. Conclusion

We have successfully fabricated the $\text{Bi}_{1-x}\text{Y}_x\text{FeO}_3$ materials with different Y doping concentration in the range from $x = 0.00$ to 0.20 by sol-gel method. The presence of BiFeO_3 rhombohedral phase in all the samples was confirmed by XRD results. The values of unit cell parameters a and c were found to decrease with increase in Y-doping. Crystallite size, which was in agreement with the XRD results, decreases as Y-doping is increased. The optical band gap of $\text{Bi}_{1-x}\text{Y}_x\text{FeO}_3$ samples deduced from the UV-vis spectra decrease with increasing Y-content. Magnetic analysis reveals ferromagnetic nature of all samples at room temperature. The remanent magnetization and the

saturation magnetization increase with increasing Y-doping concentrations. It can be concluded that the sample with 20% Y-doping has enhanced multiferroic properties with larger magnetization.

Acknowledgement

This work was supported by the National Foundation for Science and Technology Development (NAFOSTED) of Vietnam and the Research Foundation – Flanders (FWO) of Belgium (Code.FWO.2011.23). We would like to thank D.M.Thanh for some absorption measurements.

References

- [1] W. Eerenstein, N.D. Mathur, and J.F. Scott, *Nature* 442, (2006) 759 - 765.
- [2] K.S. Nalwa, A. Grag, and A. Upadhyaya, *Mater. Lett.* 62, (2008) 878.
- [3] S.T. Zhang, Y. Zhang, M.H. Lu, C.L. Du, Y.F. Chen, Z.G. Liu, Y.Y. Zhu, N.B. Ming, and X. Q. Pan, *Appl. Phys. Lett.* Vol. 88, (2006) 162901.
- [4] S. R. Das, R. N. P. Choudhary, P. Bhattacharya, R. S. Katiyar, P. Dutta, A. Manivannan, and M. S. Seehra, *J. Appl. Phys.* 101, (2007) 034104.
- [5] G.L. Yuan, and S.W. Or, *J. Appl. Phys.* 100, (2006) 024109.
- [6] G.L. Yuan, W. Siu, J.M. Liu, and Z.G. Liu, *Appl. Phys. Lett.* 89, (2006) 052905.
- [7] P. Uniyal, and K.L. Yadav, *Mater. Lett.* 62, (2008) 2858.
- [8] Hou Z.L., Zhou H.F., Yuan J., Kang Y.Q., Yang H.J., Jin H.B., and Cao M.S., *Chin. Phys. Lett.* 28, (2011) 037702.
- [9] X. Zhang, Y. Sui, X. Wang, and Y. Wang, *J. Alloys Compd.* 507, (2010) 157.
- [10] J. Xu, G. Wang, H. Wang, D. Ding, and Y. He, *Mater. Lett.* 63, (2009) 855-857.
- [11] Feng B.L., Xue H., and Xiong Z.X., *Mater. Sci.* 55, (2010) 452–456.
- [12] A. Gaur, P. Singh, N. Choudhary, D. Kumar, M. Shariq, K. Singh, N. Kaur, and D. Kaur, *Phys. B406*, (2011) 1877–1882.
- [13] Singh MK, Jang HM, Ryu S, and Jo MH, *Appl. Phys. Lett.* 88, (2006) 042907.
- [14] H. Fukumura, H. Harima, K. Kisoda, M. Tamada, Y. Noguchi, and M. Miyayama, *J. Magn. Magn. Mater.* 310, (2007) 367.
- [15] A. Gautam, K. Singh, K. Sen, R.K. Kotnala, and M. Singh, *Mater. Lett.* 65, (2011) 591-594.
- [16] M. Cazayous, D. Malka, D. Lebeugle, and D. Colson, *Appl. Phys. Lett.*, 91, (2007) 071910.
- [17] Z. Liu, Y. Qi, and C. Lu, *Mater. Electron.* 21, (2010) 380 - 384.
- [18] J. Wei, D. Xue, and Y. Xu, *Scripta Mater.* 58, (2008) 45 - 48.
- [19] M. Kumar, K.L. Yadav, and G.D. Varma, 2008. *Mater. Lett.* 62, (2008) 1159 - 1161.
- [20] K. Liu, H. Fan, P. Ren, and C. Yang, *J. Alloys Compd.* 509, (2011) 1901–1905.
- [21] A.J. Jacobson, and B.E.F. Fender, *J. Phys. C: Solid State Phys.* 8, (1975) 844.
- [22] S.V. Kiselev, R.P. Ozerov, and G.S. Zhdanov, *Sov. Phys. Dokl.* 7, (1963) 742.
- [23] Mishra R.K., Pradhan D.K., and Choudhary R N.P., *J. Phys. Condens Matter.* 20, (2008) 045218.
- [24] L. Luo, W. Wei, X. Yuan, K. Shen, M. Xu, and Q. Xu, *J. Alloys Compd.* 540, (2012) 36–38.